J Mol Model (2002) 8:150–155
DOI 10.1007/s00894-002-0081-1

ORIGINAL PAPER

**Pavla Čapková · Václav Bittner · Miroslava Trchová
Michal Ilavský**

# Molecular dynamics and IR spectroscopy in investigation of phase transitions in molecular crystal 4,4’-bis(11-hydroxy-1-undecyloxy)biphenyl

Received: 15 January 2002 / Accepted: 15 March 2002 /

**Abstract** Molecular dynamics (MD) simulations combined with temperature-dependent IR spectroscopic measurements were used to study phase transitions in molecular crystals of the mesogenic diol 4,4’-bis(11-hydroxy-1-undecyloxy)biphenyl. DSC measurements revealed four phase transitions in this molecular crystal at ~327.1 K, 389.8 K, 419.1 K and 431.9 K. Analysis of the dynamic trajectories at temperatures of 300 K, 360 K, 400 K and 480 K revealed changes in conformation of the mesogenic diol molecules and consequently changes in crystal packing and crystal structure in the temperature range 300–480 K and enabled us to understand the mechanism of the phase transitions.

**Keywords** Phase transitions · Molecular crystals · Molecular dynamics · Infrared spectroscopy · Mesogenic diol

## Introduction

Liquid crystalline polymers can be obtained from specific monomers containing mesogenic rigid segments. However, the problem in processing such polymers is the high melting point, sometimes exceeding the decomposition temperature. To decrease the phase transition temperature, flexible chain spacers between the rigid mesogenic segments are inserted. For more details about the design of thermotropic liquid crystalline polymers see, for example. [1, 2, 3, 4, 5, 6, 7, 8] Each modification of the monomers leads to changes in the thermal and mechanical properties of the polymer systems. The investigation of the structure and properties of monomers is therefore important for understanding the thermal and mechanical behavior of the derived polymer systems.

Liquid crystalline polyurethanes based on mesogenic diols and diisocyanates have been widely studied in the literature. [5, 7, 8, 9] Recently, liquid crystalline (LC) polyurethanes prepared from the mesogenic diol 4,4’-bis(6-hydroxy-1-hexyloxy) biphenyl (D) and commercial diisocyanates of various flexibilities were studied. [5, 8, 9] In these polymers complex mechanical behavior, reflecting the coupled response of the mesogenic groups to an applied force, was found. Such behavior is interesting from a practical point of view.

In the present work we investigate the mechanism of the phase transitions in molecular crystals of the mesogenic diol 4,4’-bis(11-hydroxy-1-undecyloxy)biphenyl (further denoted as D11), using a combination of molecular dynamics simulations and temperature-dependent IR spectroscopy. 4,4’-Bis(11-hydroxy-1-undecyloxy)biphenyl is shown in Fig. 1 (atoms are labeled for analysis of the bonding geometry at different temperatures). In a recent study the crystal structure of D11 was analyzed using a combination of X-ray powder diffraction, IR spectroscopy and molecular mechanics simulations. [10, 11] The structure of molecular crystals of D11 is layered, [10, 11] as one can see in Fig. 2a and b. Hydrogen bonds between the OH groups mediate the interlayer bonding. In contrast to similar molecules with shorter alkyl chains, 4,4’-bis(6-hydroxy-1-hexyloxy)biphenyl, in the case of D11 (4,4’-bis(11-hydroxy-1-undecyloxy)biphenyl) the interlayer network of hydrogen bonds is not regular because of the irregular C–C–O–H torsion at the ends of the alkyl chains. This irregularity leads to disorder in the layer stacking. [10]

An important finding was that DSC (differential scanning calorimetric) measurements revealed four distinct phase transitions (PT) in molecular crystals of D11 alone [8, 9] (see Table 1): PT-I at ~327.1 K, PT-II at ~389.9 K, PT-III at ~419.0 K and PT-IV at ~431.9 K. Qualitatively similar thermal behavior observed for linear and cross-linked polyurethanes prepared from diol D11 and molecular crystals of D11 alone suggests that investigations of

---

P. Čapková (✉) · V. Bittner · M. Trchová · M. Ilavský
Faculty of Mathematics and Physics, Charles University Prague,
Ke Karlovu 3, 12116 Prague 2, Czech Republic
e-mail: capkova@karlov.mff.cuni.cz

M. Ilavský
Institute of Macromolecular Chemistry,
Academy of Sciences of CZR, 16206 Prague 6, Czech Republic

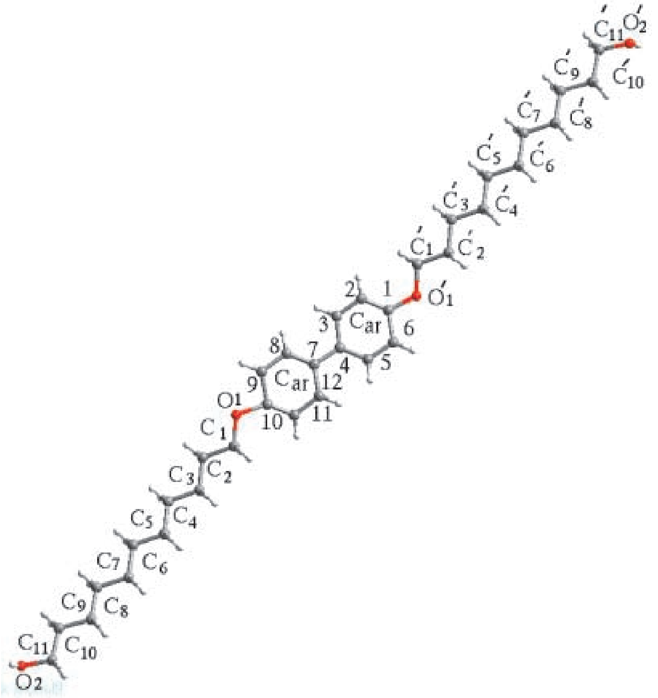

**Fig. 1** 4,4'-Bis(11-hydroxy-1-undecyloxy)biphenyl (D11)

**Table 1** The temperatures of the phase transitions in molecular crystals of 4,4'-bis(11-hydroxy-1-undecyloxy)biphenyl determined by DSC measurements

| Phase transition: | PT-I | PT-II | PT-III | PT-IV |
|---|---|---|---|---|
| *T* (K) | 327.1 | 389.9 | 419.0 | 431.9 |

structural changes in neat mesogenic diols can be important for understanding the thermal properties of the corresponding polymers. Such an investigation has been carried out in our recent study of the shorter D6 mesogenic diol 4,4'-bis(6-hydroxy-1-hexyloxy)biphenyl. [11] Molecular dynamics simulations revealed the mechanism of the phase transitions as a consequence of specific conformational changes dependent on temperature.

In the present case of the longer mesogenic diol D11 (4,4'-bis(11-hydroxy-1-undecyloxy)biphenyl), the thermal behavior is more complicated (four phase transition temperatures have been found) and our present investigation will be focused on the changes in crystal packing and unit cell dimensions induced by changes in the conformations of D11 molecules in the temperature range ~327.1–431.9 K.

## Experimental

Synthesis of 4,4'-bis(11-hydroxy-1-undecyloxy)biphenyl

Molecular crystals of 4,4'-bis(11-hydroxy-1-undecyloxy)biphenyl were prepared at the Institute of Macromolecular Chemistry, Czech Academy of Sciences. The synthesis was carried out as follows: 4,4'-bis(6-hydroxy)biphenyl (0.03 ml) was added to a solution of KOH (0.06 ml) in 200 ml of ethanol. After addition of 11-bromo-1-undecanol (0.09 mol) the mixture was stirred for 72 h at 363 K. The product was filtered off and the residue was recrystallized from a toluene/ethanol mixture mixture (1/2 by volume). After three recrystalizations a white solid product with an observed melting point of 428–429 K was obtained. Elemental

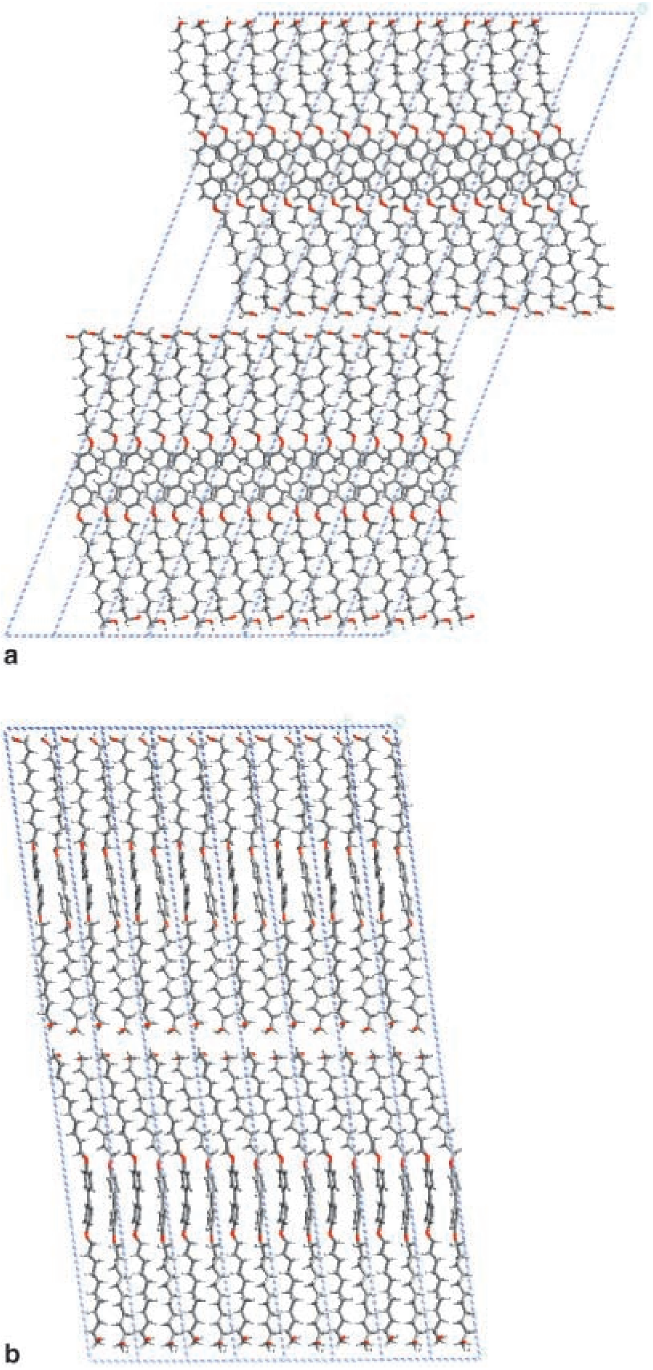

**Fig. 2a,b** View of the layered crystal structure of 4,4'-bis(11-hydroxy-1-undecyloxy)biphenyl. **a** Projection into *ac* plane. **b** Projection into *bc* plane

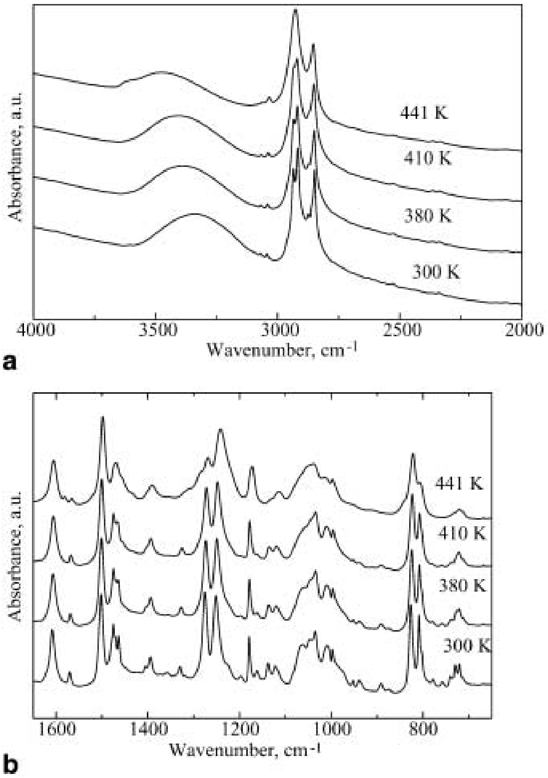

**Fig. 3** IR spectra at temperatures of 300 K, 380 K, 410 K and 441 K: **a** in the range 2000–4000 cm$^{-1}$; **b** in the range 650–1650 cm$^{-1}$

analysis for $C_{34}H_{54}O_4$ showed found/calculated values of 77.40/74.51 wt% C and 10.17/10.32 wt% H. 4,4’-Bis(11-hydroxy-1-undecyloxy)biphenyl is shown in Fig. 1.

### IR spectroscopic measurements

Vibrational spectra represent a very useful tool for the investigation of structural phase transitions in molecular crystals. Analysis of changes in vibrational modes helps to reveal the mechanism of phase transitions. (See for example. [12]) In the present work we use the analysis of vibrational spectra measured at different temperatures to support the conclusions derived from DSC measurements and modeling. The temperature dependence of the absorption spectra of 4,4’-bis(11-hydroxy-1-undecyloxy)biphenyl was measured in the range 300–441 K, on a commercial Fourier transform spectrometer Bruker IFS 66/S. All spectra in the range 500–4000 cm$^{-1}$ with 2 cm$^{-1}$ spectral resolution were obtained from compressed KBr pellets in which the samples were evenly dispersed. Two hundred scans were used to record each FTIR spectrum. The spectra were corrected for the $H_2O$ and $CO_2$ content in the optical path. The samples were electrically heated in a vacuum chamber with KBr windows. The pressure inside the chamber was 0.5 Pa. The temperature was measured using a copper–constantan thermocouple pressed against the sample.

The heating and cooling of samples was repeated twice and all spectral changes observed as a function of temperature were reproducible. The measured spectra for four different temperatures, 300 K, 380 K, 410 K and 441 K, are shown in the Fig. 3a (in the range 2000–4000 cm$^{-1}$) and in Fig. 3b (in the range 650–1650 cm$^{-1}$). The temperatures of spectroscopic measurements were chosen to catch the changes during phase transitions PT-I–IV (see above), where the phase transitions PT-III and PT-IV are so close on the temperature scale that neither spectroscopy nor molecular dynamics could distinguish between the processes accompanying this transition.

## Strategy of dynamic simulations

The initial model for dynamic simulations was built according to the crystal structure data for 4,4’-bis(11-hydroxy-1-undecyloxy)biphenyl published by van Langevelde et al. (1999). [10] The crystal structure is triclinic, space group *P1*, with unit cell parameters $a$=68.71 Å, $b$=7.43 Å, $c$=6.36 Å and $\alpha$=90.0°, $\beta$=88.53° and $\gamma$=89.57°. Dynamics simulations were carried out using the *Cerius*$^2$ modeling environment. Molecular dynamics (MD) calculations were performed on a periodic model (in the space group *P1*) and in an NPT ensemble (constant pressure/constant temperature dynamics) for 100 ps at four temperatures: 300 K, 360 K, 400 K and 480 K. The temperature was kept constant by a Berendsen thermostat. [13] The time step used in quenched dynamics was 1 fs (0.001 ps). In quenched dynamics the periods of the dynamics are followed by a quench period in which the structure is minimized (1000 steps of dynamics between quenches and 100 minimization steps in quenches). The potential energy was calculated using the pcff_300 force field, developed for polymers. [14] Atomic charges were calculated using the Qeq method (charge equilibrium approach). [15] The simulations were carried out with complete translation freedom for all atoms. MD trajectories of the system were generated with a time step of 0.001 ps over a period of 100 ps under the conditions described above.

Gavezzotti recently described [16] the application of MD simulations in the structural description of the melting process at a molecular level. The present analysis of the dynamics simulations and the interpretation of the results followed the concept of Gavezzotti. However, in addition to the structure of the molecules, we pay special attention to the consequences of the conformational behavior for the crystal packing.

## Results

### Results of IR spectroscopy

The temperature dependence of the IR spectra (see Fig. 3a and b) exhibits changes, which will be analyzed

**Table 2** Average values of the torsion angles δ and the total length $d(C_{11}–C'_{11})$ of the molecule characterizing the bonding geometry of 4,4'-bis(11-hydroxy-1-undecyloxy)biphenyl dependent on temperature; $d_{001}$ is the basal spacing (periodicity in direction perpendicular to the molecular layers), characterizing the thickness of molecular layers in the crystal

| | 300 K | 360 K | 400 K | 480 K |
|---|---|---|---|---|
| $\delta(H–O_2–C_{11}–C_{10})$ | –148(12) | +139(18) | –161(25) | –126(40) |
| $\delta(C_{ar9}–C_{ar10}–O_1–C_1)$ | –26(13) | –162(13) | +23(20) | –2.6(28) |
| $d(C_{11}–C'_{11})$ | 36.4 | 37.2 | 36.7 | 35.4 |
| $d_{001}$ | 77.4 | 80.6 | 60.5 | 69–84 |

**Table 3** The crystal structure parameters *a*, *b*, *c*, α, β, γ, cell volume *V* and density ρ at temperatures before and after phase transitions PT-I–PT-IV

| Structure parameter | 300 K | 360 K | 400 K | 480 K |
|---|---|---|---|---|
| *a* (Å) | 79.6 | 87.3 | 60.6 | 88–95 |
| *b* (Å) | 8.5 | 6.2 | 8.5 | 8.7 |
| *c* (Å) | 5.1 | 6.2 | 6.5 | 5.1 |
| α (°) | 89.9 | 89.7 | 90.6 | 90.3 |
| β (°) | 76.5 | 67.9 | 91.5 | 52–63 |
| γ (°) | 89.5 | 94.6 | 87.6 | 93.7 |
| *V* (Å$^3$) | 3380 | 3095 | 3247 | – |
| ρ (g/cm$^3$) | 1.033 | 1.132 | 1.042 | – |

with respect to the phase transitions in three temperature ranges:

1. 300–380 K corresponding to the phase transition PT-I at 327.1 K
2. 380–410 K corresponding to the phase transition PT-II at 389.9 K
3. 410–441 K corresponding to the phase transitions PT-III+IV at 419.0 and 431.9 K

Comparing the IR spectra at 300 K and 380 K in Fig. 3a and b, one can see the shift of a broad band between 3000 and 3600 cm$^{-1}$ corresponding to the ν(OH) stretching vibrations of associated hydroxyl group to higher wavenumbers. This shift indicates the partial release of interlayer hydrogen bonds due to the increasing vibrations and distortions of chain ends. This effect also leads to broadening and profile changing of the bands corresponding to the symmetric and anti-symmetric ν($CH_2$) stretching modes between 2800 and 2950 cm$^{-1}$, the deformation δ($CH_2$) and δ($O–CH_2$) vibrations of methylene groups at 1463–1475 cm$^{-1}$ and the rocking ρ($CH_2$) vibrations between 720 and 730 cm$^{-1}$. The increasing amplitude of vibrations of the chain ends also results in a change of intensity ratio of the split band at 1240–1280 cm$^{-1}$ probably corresponding to the asymmetric ν($C_{ar}$–O–C) stretching vibration and in-plane deformation β(OH) and of the band at about 1050 cm$^{-1}$ of the ν(C–OH) stretching vibration. [17] Comparison of the IR spectra at 380 and 410 K shows the growing changes described above, whereas the character of the changes remains the same as in the previous temperature range. The marked broadening and smoothing of vibration bands at 441 K indicates the pre-melting stage. The appearance of a new maximum at about 3600 cm$^{-1}$ corresponding to the monomeric hydroxyl stretching band strongly support this idea.

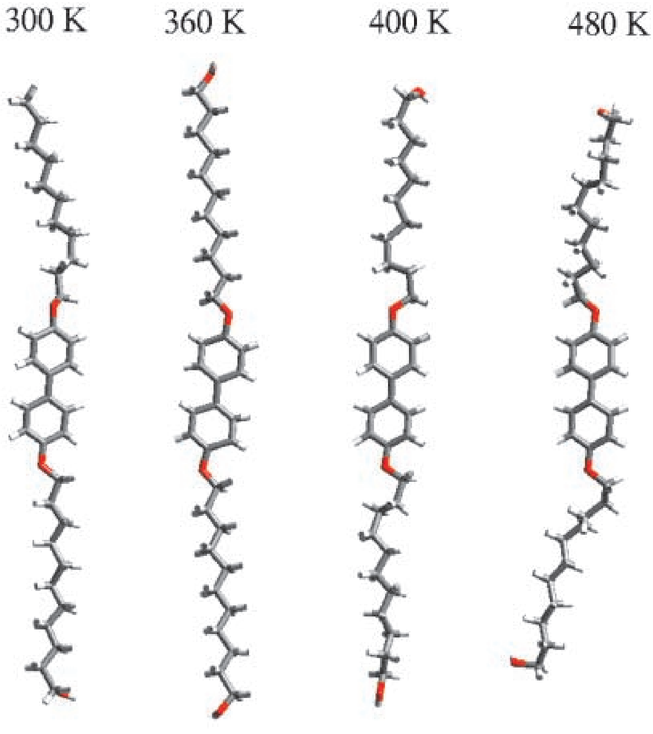

**Fig. 4** Four characteristic snapshots extracted from dynamics trajectories at temperatures of 300 K, 360 K, 400 K and 480 K, showing the main characteristic features of the conformations at a given temperature

## Results of MD simulations

The temperature dependence of the conformational behavior of D11 is illustrated in the Fig. 4, where one can see the characteristic snapshots extracted from the equilibrium part of the dynamic trajectory at temperatures of 300, 360, 400 and 480 K. Table 2 summarizes the most

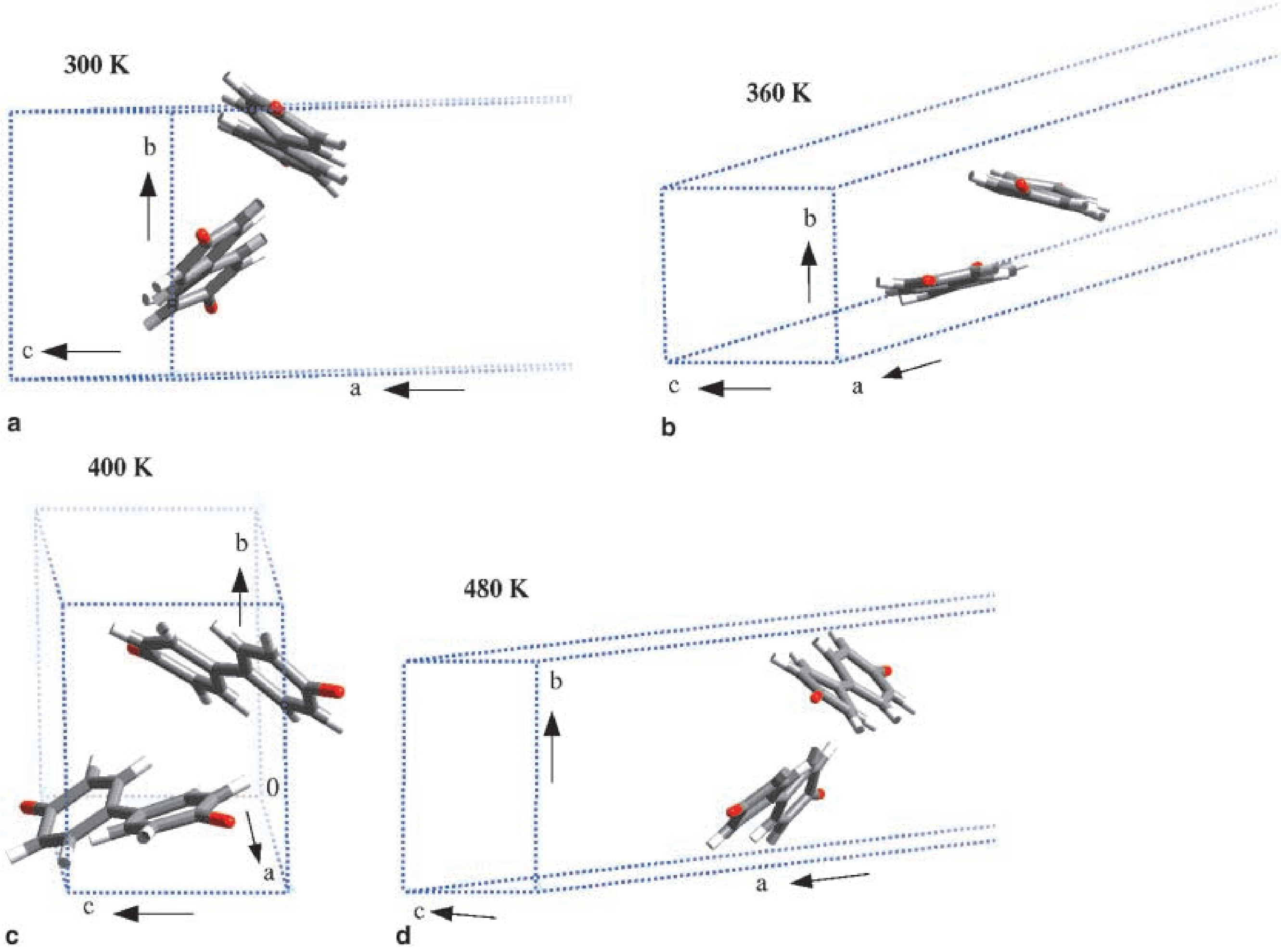

**Fig. 5** Arrangement of the biphenyl rings of D11 in the unit cell and the shape of the unit cell at the following temperatures: **a** 300 K; **b** 360 K; **c** 400 K; **d** 480 K

striking features of the temperature changes in the bonding geometry. Changes in the crystal structure parameters induced by the changes in the conformation of D11 are summarized in Table 3. The values in both tables were calculated as average values over the equilibrium part of the dynamic trajectory. The values in parenthesis represent the average vibration amplitude. The changes in crystal packing during phase transitions are illustrated in Fig. 5a–d, where one can see the position and mutual orientation of the biphenyl rings in the unit cell at temperatures of 300, 360, 400 and 480 K.

Comparing the first and second columns in Table 2, one can see the significant change in the torsion angles $\delta(\mathrm{H{-}O_2{-}C_{11}{-}C_{10}})$ and $\delta(\mathrm{C_{ar9}{-}C_{ar10}{-}O_1{-}C_1})$ during the first phase transition PT-I (at 327.1 K). This means that this phase transition is accompanied by the change in the torsion angle of the chain end and in the mutual orientation of the biphenyl rings and aliphatic chains. These changes in conformation result in changes in the molecular lengths measured as the distance between the terminal carbon atoms $C_{11}$ and $C'_{11}$. The elongation of the molecule length is accompanied by an increase of layer thickness.

These changes (illustrated in Fig. 4) are in agreement with the results of IR spectroscopy. As a result of the increasing distortions of the chain ends, the network of interlayer hydrogen bonds becomes partially broken and this effect is manifested by the shift of the band corresponding to the ν(OH) stretching vibration (3000–3600 cm$^{-1}$) to higher wavenumbers, i.e. to the band of monomeric O–H groups. More evidence for the increasing distortions in the $C_{11}H_{22}OH$ chains is the broadening and profile changing of all the bands corresponding to the $CH_2$ vibrations (see the results of IR spectroscopy). The calculated changes in torsion angles $\delta(\mathrm{H{-}O_2{-}C_{11}{-}C_{10}})$ and $\delta(\mathrm{C_{ar9}{-}C_{ar10}{-}O_1{-}C_1})$ are observable in the IR spectra as the changes in profile of the asymmetric $\nu(\mathrm{C_{ar}{-}O{-}C})$ stretching band and in-plane β(OH) deformation band and of the band at about 1050 cm$^{-1}$ corresponding to the ν(C–OH) stretching vibration. The changes in molecular shape during PT-I result in the rearrangement of molecules in the crystal structure and consequently in the change in the structure parameters, cell volume and density, as one can see in the Table 3 and Fig. 5a and b.

The second phase transition PT-II at 389 K exhibits the following characteristic changes in molecular shape (compare the columns for 360 K and 400 K). The torsion angle $\delta(H–O_2–C_{11}–C_{10})$ again exhibits dramatic changes, showing large changes in the distortion of the chain ends and in the positions and orientations of the OH groups. The pronounced change of the torsion angle $\delta(C_{ar9}–C_{ar10}–O_1–C_1)$ again indicates a large change in the mutual orientation of the biphenyl ring and $C_{11}H_{22}OH$ chain. These changes are accompanied by a shortening of the molecule ($C_{11}–C'_{11}$ distance) and a decrease of the basal spacing $d_{001}$, which corresponds to decreasing the layer thickness.

The snapshot of D11 in Fig. 4 shows clearly the large distortions of the $C_{11}H_{22}OH$ chains at 400 K after the phase transition PT-II, which results in the shrinking of the molecule and consequently in a decrease of the layer thickness. On the other hand, the rearrangement of the molecules leads to a less dense crystal packing with a higher cell volume at 400 K. The character of the IR spectra at 410 K confirms the calculated changes. The ν(OH) stretching band (3000–3600 $cm^{-1}$) is again shifted to higher wavenumbers, indicating a continuing release of interlayer hydrogen bonds. The broadening and smoothing of the $CH_2$ vibrational bands indicates larger distortions in the $C_{11}H_{22}OH$ chains. The profile change in the asymmetric $\nu(C_{ar}–O–C)$ stretching and the inplane β(OH) deformation band and of the band of the ν(C–OH) stretching mode agree with the changes in torsion angles $\delta(H–O_2–C_{11}–C_{10})$ and $\delta(C_{ar9}–C_{ar10}–O_1–C_1)$. The changes in crystal packing and crystal structure induced by the changes in the molecular shape are summarized in Table 3 and illustrated in Fig. 5c.

The phase transitions PT-III and PT-IV cannot be distinguished in the molecular dynamic simulations, as the temperature difference of 12.9 K is too small with respect to the temperature fluctuations along the dynamic trajectory. The changes in structure are therefore analyzed in the temperature range 400–480 K, which includes both phase transitions. The large vibration amplitudes of torsion angles and large fluctuations in basal spacing $d_{001}$ and $a$ parameter indicate the premelting stage, which is confirmed by the character of the IR spectrum at 441 K (the presence of the band of monomeric hydroxyl groups and possible anharmonicity of vibration). In this case the calculation of the cell volume would lead to an erroneous value.

## Conclusions

Dynamic simulations in combination with temperature-dependent IR spectroscopy revealed the changes in molecular and crystal structure of 4,4’-bis(11-hydroxy-1-undecyloxy)biphenyl dependent on temperature in the range 300–480 K. MD simulations showed that the time averaged values of bond length and angles are rather insensitive to temperature within the range 300–480 K (their variations of ~0.03 Å and max. 4.0° are within the range of thermal vibration amplitudes). The most significant and interesting changes dependent on temperature are observed for torsion angles in the $C_{11}H_{22}OH$ chains and the mutual orientation of chains and mesogenic group. These changes in the conformation of the molecules result in changes in crystal packing and crystal structure during the phase transitions. A similar mechanism of phase transitions has been observed in molecular crystals of 4,4’-bis(6-hydroxy-1-hexyloxy)biphenyl, [11] where the same combination of rigid and flexible parts of the molecule results in a similar layered crystal structure. In both crystal structures, 4,4’-bis(6-hydroxy-1-hexyloxy)biphenyl and 4,4’-bis(11-hydroxy-1-undecyloxy)biphenyl, the layers are bonded via a system of hydrogen bonds, which undergoes significant changes during phase transitions as a result of chain distortions. These changes are clearly observable in the IR spectra. The structural changes at a molecular level enable us to explain the mechanism of the phase transitions and to understand the thermal behavior of the crystal structure of 4,4’-bis(11-hydroxy-1-undecyloxy)biphenyl.

**Acknowledgements** The authors wish to thank the Grant Agency of Charles University (grants no: 37/97/B, grant 173/99, grant 166/2001/B) for financial support. The help of the Ministry of Education, Youth and Sports of the Czech Republic (grant VZ 113200002) and Grant Agency of the Academy of Sciences of the Czech republic (grant A4112901) is also greatly appreciated.

## References

1. Ciferri A, Krikbaum WR, Meyer RB (1982) Polymer liquid crystals, 1st edn. Academic Press, New York, pp 1–220
2. Donald AM, Windle AH (1992) Liquid crystalline polymer, 1st edn. Cambridge Solid State Science Series, Cambridge University Press, Cambridge, pp 51–280
3. Samulski ET (1985) Faraday Discussions of the Chemical Society, No. 79. The Faraday Division of Royal Society of Chemistry, Burlington House, London, pp 7–20
4. Chapoy LL (1983) Recent advances in liquid-crystalline polymers, 1st edn. Elsevier, London, pp 1–311
5. Ilavský M, Bouchal K, Valentová H, Lednický F, Sikora A, Baldrian J (1998) Macromol Sci Phys B37:645–666
6. Szcepaniak B, Frisch KC, Penczek P, Mejsner J, Lesczyňska I, Rudnik E (1993) J Polym Sci, Part A: Polym Chem 31:3223-3230
7. Sun SJ, Chang TC (1996) J Polym Sci, Part A: Polym Chem 34:771–779
8. Valentová H (1999) Polyurethane liquid crystalline networks and their physical properties. Thesis, Faculty of Mathematics and Physics, Charles University, Prague
9. Valentová H, Sedláková Z, Nedbal J, Ilavský M (2001) Eur Polym J 37:1511–1517
10. van Langevelde A, Čapková P, Sonneveld E, Schenk H, Trchová M, Ilavský M (1999) J Synchrotron Rad 6:1035–1043
11. Čapková P, Trchová M, Hlídek P, Schenk H, Ilavský M (2001) J Mol Struct 559:209-217
12. Baran J, Lis T, Drozd M, Ratajczak H (2000) J Mol Struct 516:185–202
13. Berendsen HJC, Postma JPM, van Gunsteren WF, DiNola A, Haak JR (1984) J Chem Phys 81:3684–3690
14. Sun H, Mumby SJ, Maple JR, Hagler AT (1994) J Am Chem Soc 116:2978–2987
15. Rappé AK, Goddard III WA (1991) J Phys Chem 95:3358–3363
16. Gavezzotti A (1999) J Mol Struct 485–486:485–499
17. Socrates XG (1980) Infrared characteristic group frequencies, 1st edn. Wiley, Chichester